

A New Scheme for Determination of Respiration Rate in Human Being using MEMS Based Capacitive Pressure Sensor: Simulation Study

Madhurima Chattopadhyay

Dept. of Applied Electronics and Instrumentation
Engineering, Heritage Institute of Technology,
Kolkata: 700 107, India
E-mail: madhurima02@gmail.com

Deborshi Chakraborty

Department of Instrumentation Science, Jadavpur University,
Kolkata: 700 032, India
E-mail: dcphy123@gmail.com

Abstract— In this paper, a MEMS based capacitive nasal sensor system for measuring Respiration Rate (RR) of human being is developed. At first two identical diaphragm based MEMS capacitive nasal sensors are designed and virtually fabricated. A proposed schematic of the system consists of signal conditioning circuitry alongwith the sensors is described here. In order to measure the respiration rate the sensors are mounted below Right Nostril (RN) and Left Nostril (LN), in such a way that the nasal airflow during inspiration and expiration impinge on the sensor diaphragms. Due to nasal airflow, the designed square diaphragm of the sensor is being deflected and thus induces a corresponding change in the original capacitance value. This change in capacitance value is to be detected by a correlated-double-sampling (CDS) capacitance-to-voltage converter is designed for a precision interface with a MEMS capacitive pressure sensor, followed by an amplifier and a differential cyclic ADC to digitize the pressure information. The designed MEMS based capacitive nasal sensors is capable of identifying normal RR (18.5 ± 1.5 bpm) of human being. The design of sensors and its characteristics analysis are performed in a FEA/BEA based virtual simulation platform.

Index Terms— MEMS capacitive nasal sensor, diaphragm deflection, respiration rate (RR), oscillator, sensitivity, Finite Element Analysis, Boundary Element Analysis.

I. INTRODUCTION

Respiratory Rate (RR) is a very important physiological parameter to be monitored in people both in healthy and critical condition, as it gives meaningful information regarding their respiratory system performance as well as condition [1]. The RR is defined as the number of breaths per minute [2]. A typical RR at resting is 12 and its corresponding frequency is 0.2 Hz [2]. During recovery from surgical anesthesia, a μ -opioid agonists used for pain control can slow down RR leading to bradypnea ($RR < 12$) or even apnea (cessation of respiration for an indeterminate period) [3], while airway obstructions like asthma, emphysema and COPD will increase RR causing tachypnea ($RR > 30$) [4]. Hence, RR measurement becomes clinically very important. The methods commonly used for measuring RR are visual observation, impedance pneumography, acoustic sensing, fiber optic sensing, Respiratory Inductance Plethysmograph (RIP) and nasal prongs (NP) [5]. However, due to very sensitive patients' movements and high cost, these methods find limited use in the clinical settings [6]. Earlier, Siivola [8], Choi and Jiang[8,9]

used Poly Vinyl Di Fluoride (PVDF) to record respiration and cardiac action in human beings. In 2008, J.H. Oum et al. reported a non contact type capacitive sensor for determination of the heart rate and respiration rate [10]. Different materials have been studied as a diaphragm material for such capacitive sensors and it has been reported that Polysilicon is working efficiently as diaphragm material for a wide variety of applications [7].

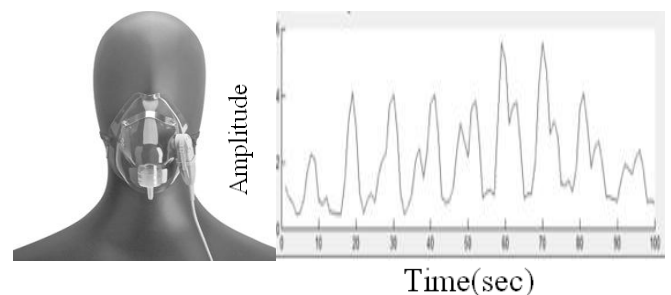


Fig. 1. Schematic of the process for the respiration rate (RR) measurement

In our present study, MEMS based capacitive respiration rate sensor is designed in FEA/BEA based virtual design simulation platform. The characteristics analysis of the designed sensor is also computed in the same simulation software. The characteristics plots obtained from the sensor are compared with 'Gold standard' RIP and NP methods.

II. SENSOR DESIGN

Fig. 2 illustrates the innovative design of the square shaped diaphragm based MEMS capacitive pressure sensor for determination of the respiration rate (RR). As shown in the Fig. 2, this capacitive pressure sensor consists of a pair of plates (one fixed plate and one moving plate). The diaphragm, the moving plate and the fixed plate are all in square shape to maintain mirror symmetry for the stresses at the edges where the diaphragm is clamped.

The fixed plate is placed in parallel with the moving plate to form a parallel plate capacitor. This fixed plate also caps the moving plate inside of a sealed cavity.

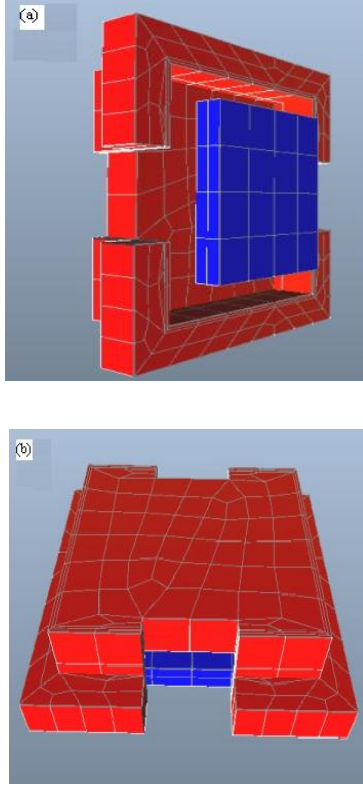


Fig. 2. 3D view of the designed respiratory sensor (a) Top view and (b) Side View

As the diaphragm deflects under a pressure load, the moving plate of the capacitor experiences the same amount of deflection from the center of the diaphragm. Thus a diaphragm deflection is readily converted to a capacitance change. For square diaphragm with a small deflection at any point(x,y) is given by[11]:

$$w(x,y) = \frac{49Pa^4(x^2-a^2)(y^2-a^2)}{2304D} \quad (1)$$

Here, 'a' is the half side length of the diaphragm and maximum deflection occurs at the center (x=0, y=0) is given by

$$w_0 = \frac{0.216Pa^4}{Fh^3} \quad (2)$$

and the capacitance is given as:

$$C = \iint \frac{\epsilon dx dy}{d - w(x,y)} \quad (3)$$

Here, in this simulation platform Eq.(3) is solved numerically. For a small deflection, the analytical deflection of the capacitance can be derived by expanding the denominator of Eq. (3) in the Taylor's series expansion as given below:

$$C = \frac{\epsilon}{d} \iint \left\{ 1 + \frac{w(x,y)}{d} + \frac{w^2(x,y)}{2d^2} \right\} dx dy \quad (4)$$

Since it is a small deflection case the higher order terms in the expression can be neglected and the Eq. (4) reduces to:

$$C = \frac{\epsilon}{d} \iint \left\{ 1 + \frac{w(x,y)}{d} \right\} dx dy \quad (5)$$

Integrating eq. (5) and using the value of w(x,y) from eq. (1) we get,

$$C = C_0 \left(1 + \frac{12.5Pa^4}{2025dD} \right) \quad (6)$$

Here, in this simulation platform Eq.(6) is solved numerically. Where, C_0 is the zero pressure capacitance and is given by,

$$C_0 = \epsilon 4a^2/d \quad (7)$$

The term sensitivity of a capacitive type pressure sensor can be defined as,

$$S_A = \frac{dC}{dP} \quad (8)$$

Thus, sensitivity is obtained in this work by differentiating Eq. (6) w.r.t. pressure (P) and can be expressed as

$$S_A = \frac{49 \epsilon a^6}{2025d^2D} \quad (9)$$

III. VIRTUAL SENSOR FABRICATION

The virtual fabrication steps for the designed sensor in FEA/BEA based virtual simulation software is provided below.

We have chosen Si Czochralski (100) as a substrate material with thickness of 10 (μm) (Fig. 3(1)). Then a thin layer of SiO₂ is deposited over the substrate (Fig. 3(2)). The thickness of this layer is of 1000 nm (Conformal). A photo resist (PR-AZ5214) is deposited via spin coating technique having thickness of 300 nm (Fig. 3(3)).

Now the UV Lithography is performed with Mask as shown in Layer 1 (Fig. 3(4)). Partial Etching of SiO₂ layer has been done with Wet (BOE) (Fig. 3(5)). Again wet etching is applied to remove the photo resist PR-AZ5214 (Fig. 3(6)).

In order to design the fixed plate, P Implant (P-ion) is doped with a junction depth of 1000 nm (Fig. 3(7)). Hence wet etching has been taken place to remove SiO₂ (Fig. 3(8)).

A sacrificial layer of PSG (Phosphosilicate Glass) is deposited on the fixed plate by LPCVD (Fig. 3(9)). Once the sacrificial layer thickness 2000 nm (Conformal) is formed, the photo resist (PR-AZ5214) is again deposited (Fig. 3(10)).

Subsequently, to generate the cap type upper plate lithography with UV Contact is performed with Mask Layer 2 (Fig 3(11)). As we have applied negative resist,

The side walls are removed leaving behind the middle portion where the mask is placed.

Now PolySi is deposited by LPCVD of thickness 1000 nm (Conformal) in order to form upper movable diaphragm (Fig. 3(14)). Moreover to achieve the desired shape, Mask Layer 3 is placed over the layer of polySi and UV Lithography was performed (Fig. 3(16)).

Reactive Ion Etching (RIE) using Cl₂ has applied to remove the extra deposited layers of PolySi from the side surfaces (Fig. 3(17)).

Again PR-AZ5214 is removed by Wet Etching (Fig. 3(18)). The required gapping between the two plates is achieved by etching out the PSG layer. Simultaneously, the photo resist is also removed Etch PSG Generic (Fig. 3(19)).

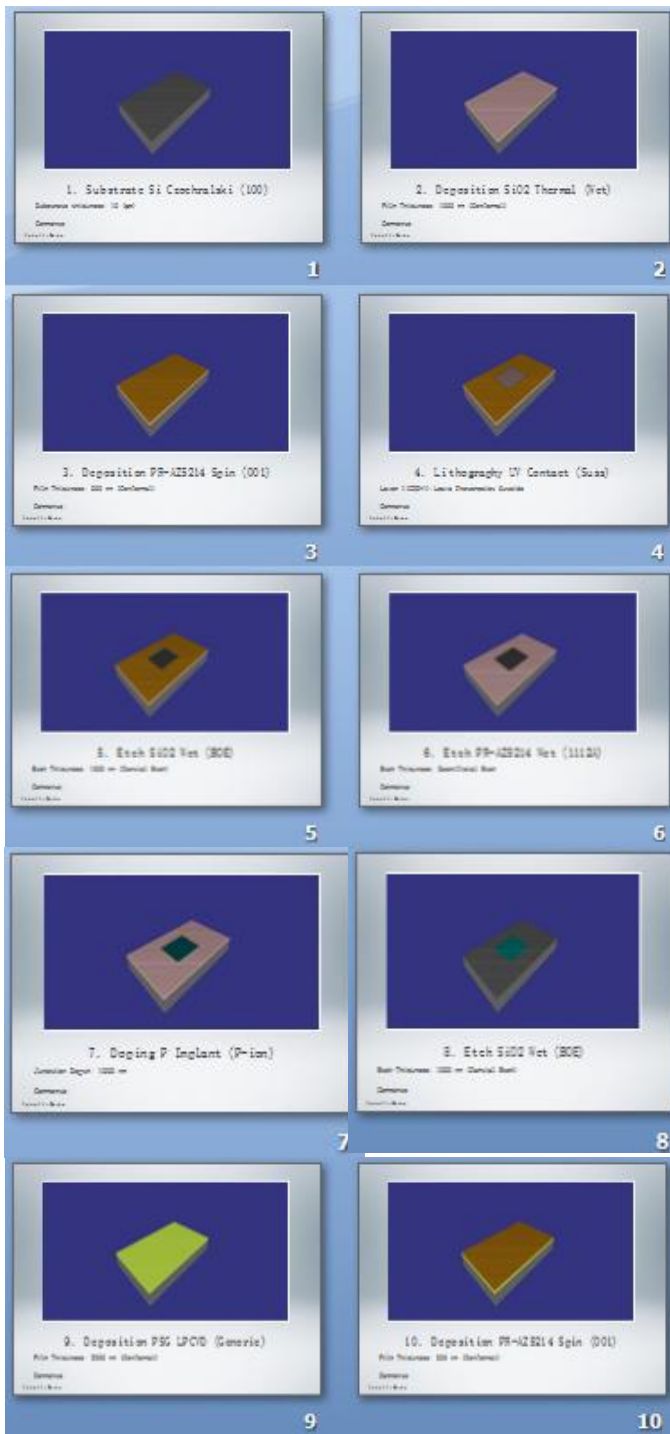


Fig. 3. Views of the virtually fabricated sensor with the above mentioned steps.

Finally, Sacrificial Si is removed through wet (HNO₃_HF): Etching (Fig. 3(20)).

The designed mask layers for virtually fabrication of the sensor is shown in Fig. 4.

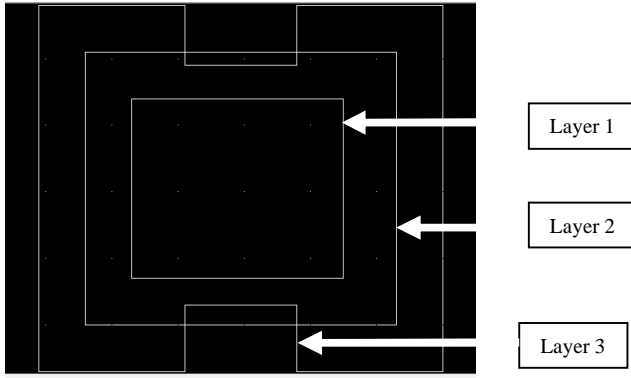


Fig. 4. Design of the mask layers in the simulation platform

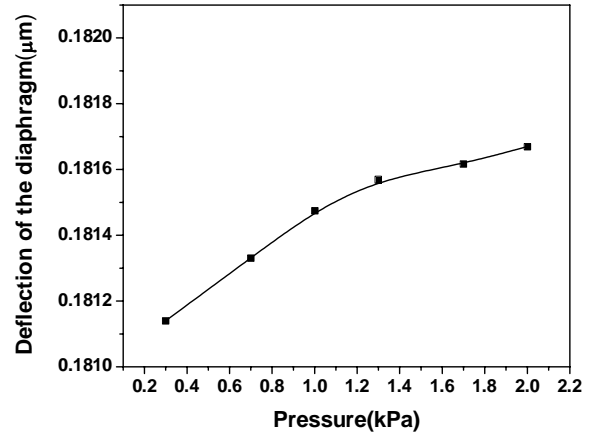


Fig. 6. Plot of deflection of the diaphragm corresponding to the pressure (0.2-2.2 kPa)

IV. RESULT AND DISCUSSIONS

The pressure range during exhalation for a healthy human being varies from 0.3 kPa to 2 kPa. Therefore pressure range mentioned before is applied on the diaphragm of the designed sensor. Corresponding deflection of the diaphragm for a minimum and maximum pressure of that specified pressure range if given in Fig. 5 (a,b) and its corresponding plot for the whole pressure range is shown in Fig. 6.

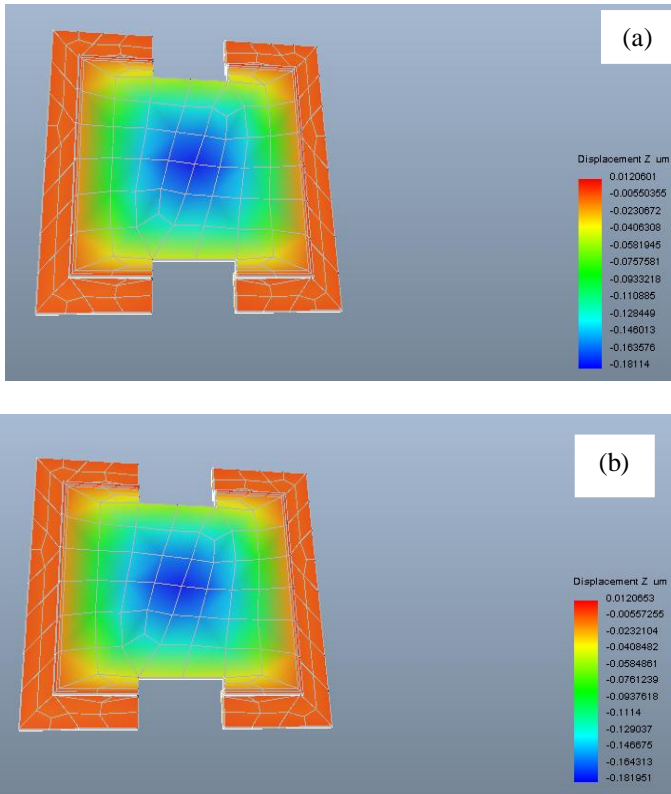


Fig. 5. Simulated view of the diaphragm displacement with applied pressure of (a) 0.3 kPa (b) 2 kPa

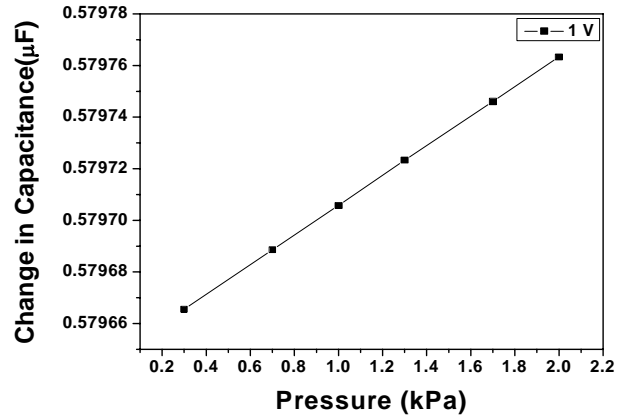


Fig. 7. Plot of Change in capacitance (μF) vs. Pressure (kPa)

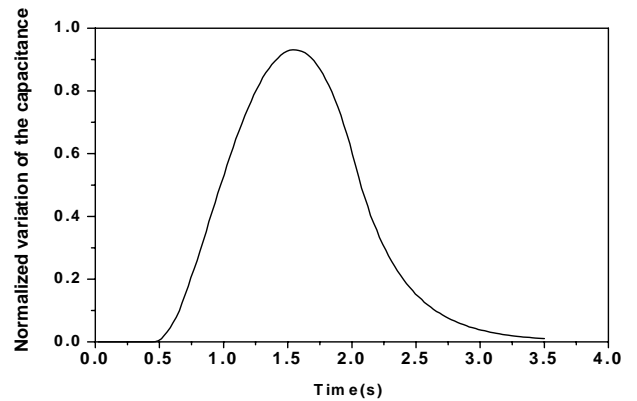


Fig. 8. Dynamic response of the diaphragm

The change in capacitance (μF) with applied pressure of 0.3-2 kPa for a potential of 1 Volt applied between the plates is shown in Fig. 6. It gives a linear response for the exhaled pressure range. In order to detect the exhalation rate, the

corresponding movement of the diaphragm due to the applied pressure, induces a change in the capacitance between the plates with respect to time. As a result, the dynamic response of the designed sensor is obtained for the range of the exhaled pressure which is represented in Fig.7. It is observed that the pattern obtained from the response validate with the normal breathing rate (18.5 ± 1.5 bpm) of the human being [12].

V. CONCLUSIONS

In this present study we have restricted our work in simulation only where we have verified the simulation studies with the actual exhaled pressure. During verification, the nature of the dynamic response is showing a confirmation with the actual nature of the normal breathing pattern, a more detailed study on different RR (number of breaths per minute (bpm)) corresponding to tachypnea (34.5 ± 4 bpm), and bradypnea (10.5 ± 2.2 bpm) will be performed. Once the simulation study will be satisfied, a real time implementation of this system will be developed with required associated signal conditioning circuitry.

VI. FUTURE IMPLEMENTATION

The Fig. 9 presents overall block diagram of the electronic system design architecture for the signal processing of the sensor. A fully differential architecture is chosen for the interface electronics to suppress common-mode disturbances. A correlated-double-sampling (CDS) capacitance-to-voltage converter is designed for a precision interface with a MEMS capacitive pressure sensor, followed by an amplifier and a differential cyclic ADC to digitize the pressure information.

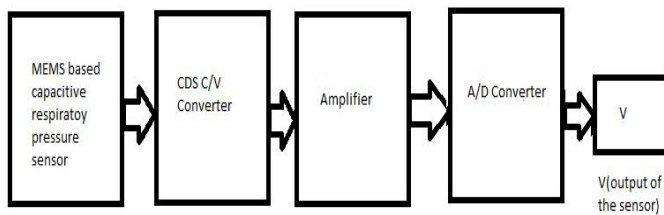


Fig. 9. Block diagram of the electronic system design architecture of the MEMS capacitive type nasal exhalation sensor

The obtained output in the form of voltage is calibrated with the respiration rate pressure and is stored for the further analysis..

ACKNOWLEDGMENT

Author Madurima Chattopadhyay likes to acknowledge Department of Science and Technology, Govt. of India for financial support from the First Track Young Scientist scheme to carry out the research work.

REFERENCES

- [1] Milic-Emili J, "Recent advances in clinical assessment of control of breathing", *Lung* 1982, pp. 160:1 – 17.
- [2] D. Moffett, S. Moffett and C. Schauf, "Human physiology", 2nd edition, Wm. C. Brown Publishers, 1993, Ch. 13 and 16.
- [3] Ivana Prkic et al., "Pontine μ -opioid receptors mediate bradypnea caused by intravenous remifentanyl infusions at clinically relevant concentrations in dogs," *J Neurophysiol* 2012, vol.108, pp. 2430 –2441.
- [4] Weigt SS, Abrazado M, Kleerup EC, Tashkin DP, Cooper CB, "Time course and degree of hyperinflation with metronome-paced tachypnea in COPD patients," *COPD* 2008, vol. Oct;5(5), pp.298-304. doi: 10.1080/15412550802363428.
- [5] Folke M, Cernerud L, Ekstrom M, Hok B, "Critical review of non-invasive respiratory monitoring in medical care," *Med Biol Eng Comput* 2003, vol. 41, pp.377-383.
- [6] R. Farre , J.M. Montserrat, D. Navajas, "Noninvasive monitoring of respiratory mechanics during sleep," *Eur Respir J* 2004, vol. 24, pp. 1052–1060.
- [7] H.Kawai, "The piezoelectricity of Polyvinylidene fluoride", *J. appl.phys.* 1969, vol.,8, pp.73-77.
- [8] Siivola J, "New non-invasive piezoelectric transducer for recording of respiration, heart rate and body movements. *Med Bio Eng Comp* 1989, vol. 27, pp.423-424.
- [9] Choi S, Jiang Z., "A novel wearable sensor device with conductive fabric and PVDF film for monitoring cardiorespiratory signals," *Sensors and Actuators A: Physical* 2006, vol. 128, pp.317-326.
- [10] J.H. Oum, S.E. Lee, D.-W. Kim and S. Hong, "Non-contact heartbeat and respiration detector using capacitive sensor with Colpitts oscillator", *ELECTRONICS LETTERS* 17th January 2008 Vol. 44 No. 2.
- [11] Anurekha Sharma, "Modelling of a Pull-in voltage and touch point pressure for MEMS capacitive transducers with square diaphragm", Kurukshetra University, Kurukshetra., Ph.D. thesis July 2008.
- [12] Roopa et al., "Identification of different respiratory rate by a piezo polymer based nasal sensor", *IEEE Explore* 978-1-4673-4642-9/13.